



Contents lists available at ScienceDirect

## Journal of Quantitative Spectroscopy and Radiative Transfer

journal homepage: [www.elsevier.com/locate/jqsrt](http://www.elsevier.com/locate/jqsrt)MARVEL analysis of high-resolution rovibrational spectra of  $^{17}\text{O}^{13}\text{C}^{18}\text{O}$  and  $^{17}\text{O}^{13}\text{C}^{17}\text{O}$ Ala'a A.A. Azzam <sup>b</sup>,\* Joud M.A. AlAlawin <sup>a</sup>, Jonathan Tennyson <sup>c</sup>,\* Tibor Furtenbacher <sup>d</sup>, Attila G. Császár <sup>d</sup><sup>a</sup> Research Department, AstroJo Institute, Wasfi Al-Tal St, Amman, Jordan<sup>b</sup> Department of Physics, The University of Jordan, Queen Rania St, Amman, Jordan<sup>c</sup> Department of Physics and Astronomy, University College London, Gower Street, London WC1E 6BT, UK<sup>d</sup> ELTE Eötvös Loránd University, Institute of Chemistry, H-1117 Budapest, Pázmány Péter sétány 1/A, Hungary

## ARTICLE INFO

## Keywords:

Rovibrational energy levels

CO<sub>2</sub> $^{17}\text{O}^{13}\text{C}^{18}\text{O}$  $^{17}\text{O}^{13}\text{C}^{17}\text{O}$ 

Line positions

Transitions

MARVEL

## ABSTRACT

Spectroscopic networks, based on rovibrational line-center measurements found in 10/5 literature sources, are presented for the triply substituted carbon dioxide isotopologues  $^{17}\text{O}^{13}\text{C}^{18}\text{O}/^{17}\text{O}^{13}\text{C}^{17}\text{O}$  (738/737, according to a well-established shorthand notation followed in this study). For 738/737, the spectroscopic networks contain 2058(1488)/1831(1349) measured(unique) transitions, belonging to 25/22 vibrational bands. The transitions collected for 738 and 737 span the wavenumber regions 623–7888 and 624–6739  $\text{cm}^{-1}$ , respectively. These spectroscopic networks determine 945 and 877 empirical rovibrational energy levels for 738 and 737, respectively, extracted with the help of the MARVEL (Measured Active Rotational–Vibrational Energy Levels) protocol and code. The energy levels of 738/737 span the range of 0–8762/0–7201  $hc\text{ cm}^{-1}$  and the polyads from 0 to 11 for 738 and from 0 to 10 for 737. A detailed comparison of the empirical rovibrational energy levels of this study with their counterparts in two published databases, CDS-296, and Ames-2021, shows very good overall agreement.

## 1. Introduction

Despite being just a trace gas in the Earth's atmosphere, carbon dioxide, CO<sub>2</sub>, influences our planet's radiation balance significantly [1–5]. The rising concentration of CO<sub>2</sub> in the Earth's atmosphere, due mainly to fossil fuel combustion, impacts our ecosystem and the climate, as well [6]. A key characteristic of CO<sub>2</sub>'s atmospheric presence is the variation of its concentration over time [7]. Understanding the spectroscopic properties of CO<sub>2</sub> [8,9], including the line center positions of the rovibrational transitions of particular interest for this study, is essential for measuring accurately CO<sub>2</sub> abundance and distribution in different environments, from the tropics to the poles. These data are crucial for studying climate change and atmospheric radiative balance [10]. Remote sensing missions, like NASA's OCO-2 and OCO-3 [4] and ESA's CO2M [11] rely on the availability of highly accurate spectroscopic data. Similarly, ground-based networks, such as TCCON (Total Carbon Column Observing Network), provide essential measurements for monitoring atmospheric CO<sub>2</sub> with increasing accuracy [12].

Since the main isotopologue of CO<sub>2</sub>,  $^{16}\text{O}^{12}\text{C}^{16}\text{O}$  (626 in a shorthand notation introduced by HITRAN [13]), has saturated absorption bands, spectroscopic characterization of minor carbon dioxide isotopologues becomes especially important [14,15]. The optically thin absorption features of carbon dioxide isotopologues allow for precise spectroscopic measurements, making them valuable for tracking atmospheric CO<sub>2</sub> variations. Although these isotopologue transitions contribute minimally to radiative forcing, they possess distinct absorption lines that are useful for tracing CO<sub>2</sub> sources and understanding atmospheric dynamics. This enhances climate studies and atmospheric monitoring efforts.

The present study focuses on rovibrational spectra measured, under various conditions, by a number of different techniques, for the eleventh and twelfth most abundant carbon dioxide isotopes,  $^{17}\text{O}^{13}\text{C}^{18}\text{O}$  and  $^{17}\text{O}^{13}\text{C}^{17}\text{O}$  (with HITRAN codes 738 and 737, respectively). A significant number of high-resolution spectroscopic studies are available for both rare isotopologues [16–25]. Our main goal is to provide expansive spectroscopic datasets for the 738 and 737 isotopologues.

\* Corresponding authors.

E-mail addresses: [alaa.azzam@ju.edu.jo](mailto:alaa.azzam@ju.edu.jo) (A.A.A. Azzam), [j.tennyson@ucl.ac.uk](mailto:j.tennyson@ucl.ac.uk) (J. Tennyson).<https://doi.org/10.1016/j.jqsrt.2025.109485>

Received 16 March 2025; Received in revised form 21 April 2025; Accepted 21 April 2025

Available online 2 May 2025

0022-4073/© 2025 The Author(s). Published by Elsevier Ltd. This is an open access article under the CC BY license (<http://creativecommons.org/licenses/by/4.0/>).

**Table 1**

Some characteristics of validated rovibrational transition datasets used in our MARVEL studies of the 12 stable isotopologues of carbon dioxide [36–42] compared to those of two spectroscopic databases, CDS-296 [43] and HITRAN 2020 [13].  $N_{\text{tot}}$  = the total number of transitions.  $N_{p-p}$ ,  $N_{o-o}$ , and  $N_{p-o}$  are the number of transitions within the *para* (*p*) and *ortho* (*o*) principal components of the spectroscopic networks. TW = this work.

Isotopologue	MARVEL				CDS-296 [43]				HITRAN 2020 [13]			
	$N_{\text{tot}}$	$N_{p-p}$	$N_{o-o}$	$N_{p-o}$	$N_{\text{tot}}$	$N_{p-p}$	$N_{o-o}$	$N_{p-o}$	$N_{\text{tot}}$	$N_{p-p}$	$N_{o-o}$	$N_{p-o}$
$^{16}\text{O}^{12}\text{C}^{16}\text{O}$ (626) [36]	44 821	44 821	–	–	282 708	282 708	–	–	171 604	171 604	–	–
$^{16}\text{O}^{13}\text{C}^{16}\text{O}$ (636) [37]	20 790	20 790	–	–	301 611	301 611	–	–	69 749	69 749	–	–
$^{16}\text{O}^{12}\text{C}^{18}\text{O}$ (628) [38]	33 658	12 661	12 602	8395	690 531	251 720	251 720	187 272	121 970	47 729	47 748	26 493
$^{16}\text{O}^{12}\text{C}^{17}\text{O}$ (627) [39]	16 225	6 691	6 705	2829	632 995	249 198	249 092	134 705	73 899	31 411	31 396	11 092
$^{16}\text{O}^{13}\text{C}^{18}\text{O}$ (638) [40]	13 384	5 596	5 689	2099	737 955	270 190	269 998	197 767	41 048	17 068	17 036	6944
$^{16}\text{O}^{13}\text{C}^{17}\text{O}$ (637) [42]	5 050	2 279	2 266	505	670 253	264 361	264 327	141 565	23 608	10 736	10 723	2149
$^{18}\text{O}^{12}\text{C}^{18}\text{O}$ (828) [41]	11 653	11 653	–	–	301 985	301 985	–	–	10 498	10 498	–	–
$^{17}\text{O}^{12}\text{C}^{18}\text{O}$ (728) [41]	11 340	4 835	4 840	1665	649 258	256 902	256 859	135 497	14 624	6 806	6 793	1025
$^{17}\text{O}^{12}\text{C}^{17}\text{O}$ (727) [42]	10 252	4 950	5 302	–	506 092	244 489	261 603	–	6 494	3 075	3 419	–
$^{18}\text{O}^{13}\text{C}^{18}\text{O}$ (838) [41]	2 425	2 425	–	–	321 105	321 105	–	–	2 927	2 927	–	–
$^{17}\text{O}^{13}\text{C}^{18}\text{O}$ (738) [TW]	2 057	1 075	982	–	687 927	273 850	273 735	140 342	3 981	1 975	1 978	28
$^{17}\text{O}^{13}\text{C}^{17}\text{O}$ (737) [TW]	1 822	901	921	–	542 412	261 727	280 685	–	1 502	710	792	–

**Table 2**

The number of empirical (MARVEL) rovibrational energy levels determined by our group for the twelve stable isotopologues of carbon dioxide [37–42], and the maximum absolute (MAD) and average absolute (AAD) energy level differences,  $\Delta E$ , in  $hc\text{ cm}^{-1}$ , between the MARVEL studies and those from Ames-2021 [34] and CDS-296 [43]. Nat. abund. = natural abundance as given by HITRAN [13], TW = this work.

Isotopologue	Nat. abund.	No. of energy levels	$\Delta E_{\text{Ames-2021}}^{\text{MAD}}$	$\Delta E_{\text{Ames-2021}}^{\text{AAD}}$	$\Delta E_{\text{CDS-296}}^{\text{MAD}}$	$\Delta E_{\text{CDS-296}}^{\text{AAD}}$
$^{16}\text{O}^{12}\text{C}^{16}\text{O}$ (626) [36]	$9.842 \times 10^{-1}$	8268	0.147	0.015	0.077	0.001
$^{16}\text{O}^{13}\text{C}^{16}\text{O}$ (636) [37]	$1.106 \times 10^{-2}$	6318	0.152	0.016	0.081	0.002
$^{16}\text{O}^{12}\text{C}^{18}\text{O}$ (628) [38]	$3.947 \times 10^{-3}$	8786	0.231	0.022	0.182	0.002
$^{16}\text{O}^{12}\text{C}^{17}\text{O}$ (627) [39]	$7.340 \times 10^{-4}$	5036	0.085	0.012	0.009	0.001
$^{16}\text{O}^{13}\text{C}^{18}\text{O}$ (638) [40]	$4.434 \times 10^{-5}$	3975	0.151	0.024	0.268	0.002
$^{16}\text{O}^{13}\text{C}^{17}\text{O}$ (637) [42]	$8.246 \times 10^{-6}$	1960	0.087	0.014	0.033	0.001
$^{18}\text{O}^{12}\text{C}^{18}\text{O}$ (828) [41]	$3.957 \times 10^{-6}$	3923	0.571	0.042	0.559	0.002
$^{17}\text{O}^{12}\text{C}^{18}\text{O}$ (728) [41]	$1.472 \times 10^{-6}$	4318	0.109	0.024	0.046	0.001
$^{17}\text{O}^{12}\text{C}^{17}\text{O}$ (727) [42]	$1.368 \times 10^{-7}$	3278	0.105	0.017	0.017	0.001
$^{18}\text{O}^{13}\text{C}^{18}\text{O}$ (838) [41]	$4.446 \times 10^{-8}$	1058	0.168	0.045	0.039	0.001
$^{17}\text{O}^{13}\text{C}^{18}\text{O}$ (738) [TW]	$1.654 \times 10^{-8}$	945	0.123	0.029	0.014	0.001
$^{17}\text{O}^{13}\text{C}^{17}\text{O}$ (737) [TW]	$1.538 \times 10^{-9}$	877	0.071	0.018	0.008	0.001

In addition to that, this study is distinguished by two important features. The first one is the use of accurately measured, validated line positions with unique lower- and upper-state labels, while the second one is the determination of empirical rovibrational energies with experiment-based uncertainties. Determination of the energy levels from the measured transitions is accomplished through the use of the MARVEL (Measured Active Rotational–Vibrational Energy Levels) procedure [26–30], which is based on the theory of spectroscopic networks [31,32]. The resulting datasets can be used to refine line lists such as those provided by HITRAN [13], NASA Ames [33,34], and ExoMol [35], and support variational nuclear motion calculations. This work is part of our systematic investigation of carbon dioxide isotopologues, with results published for 626 [36], 636 [37], 628 [38], 627 [39], 638 [40], 838 [41], 728 [41], 828 [41], 637 [42], and 727 [42].

Since this study completes our MARVEL analysis of the high-resolution spectra of the 12 stable isotopologues of carbon dioxide, we also provide a brief summary of the validated measured transitions of these 12 isotopologues in Tables 1 and 2, which concentrate on transitions and energy levels, respectively. Table 1 compares characteristics of measured transitions used in MARVEL with entries in the CDS-296 [43] and HITRAN 2020 [13] datasets. Comparing the total number of transitions in the three datasets shows very clearly the lack of experimental measurements and how nuclear spin isomerism affects the distribution of the transitions within the various isotopologues. Statistical measures concerning the empirical rovibrational energies determined in our studies, with respect to the NASA Ames-2021 [34] and the Carbon Dioxide Spectroscopic Databank (CDS-296) [43] datasets of energy levels, are listed in Table 2, and show that the empirical energy levels agree with their CDS-296 counterparts by an order of magnitude better for all isotopologues.

## 2. Theoretical background

### 2.1. MARVEL

MARVEL [26–30,44] is a tool which can be used to efficiently validate and analyze high-resolution spectroscopic line position measurements and invert the information contained in them to determine empirical energy levels. MARVEL works through the construction of a “spectroscopic network” (SN) [31,32], where the energy levels form a set of vertices, the transitions between them are the edges, and different vertex and edge weights can be applied.

When transition measurements are collected for a MARVEL analysis, one must ensure that each line has an accurate center position with an associated uncertainty (the uncertainties of our input datasets are interpreted as expanded uncertainties with coverage factor  $k = 2$ , roughly corresponding to a 95% confidence interval), and that the upper and lower energy levels involved in the transition are labeled uniquely. Based on the spectroscopic network created, MARVEL can identify most of the inconsistencies in the transition dataset and, based on the validated transitions, it yields empirical energy levels through an inversion protocol. Following the standard notation of graphs and networks [45], a component of the SN refers to a self-contained set of energy levels (vertices) interconnected through observed spectroscopic transitions (edges). By definition, these components form isolated sub-networks within the complete spectroscopic network and remain disconnected due to symmetry reasons (e.g., nuclear spin isomerism, leading to so-called principal components) or unobserved transitions (leading to so-called floating components) [29]. One of the principal components contains the root of the SN, that is the lowest-energy quantum state of the molecule. The floating components [29] can be connected to the root and the measured transitions using sufficiently accurate semi-empirical data (coming from perhaps effective Hamiltonian fits) or, for

some molecules, by using the known quasi-degeneracy of certain highly excited quantum states [46].

Variational quantum-chemical approaches solving the nuclear Schrödinger equation yield energy levels with rather limited accuracy when compared to spectroscopic measurements, even when the potential energy surface is extremely close to the complete basis set full configuration interaction limit [47,48]. In contrast, the accuracy of the empirical (MARVEL) energy levels is not restricted by assumptions other than the validity of the Ritz principle [49] and, of course, the accuracy of the measurements. This allows the transfer of experimental accuracy to the empirical energy levels during a MARVEL analysis. There is an important caveat, however, namely that this also allows MARVEL to accept transitions that might break standard quantum-mechanical selection rules or are incorrect otherwise, as long as the transition is not in conflict with other entries in the dataset. Comparisons with independent (theoretical) sources of energy levels can be used to identify such problems.

In this study, we used the latest version of the MARVEL code, MARVEL4 [44]. MARVEL4 has an option to use an adaptation of the bootstrap method to give final uncertainties for the energy levels; our final energy levels are given with expanded uncertainties obtained using this procedure.

## 2.2. Rovibrational quantum numbers

As noted above, MARVEL knows nothing about the detailed rules of quantum mechanics. Thus, to ensure a meaningful validation of the measured transitions during a MARVEL run, it is essential to keep energy level labeling consistent across the dataset (though this in itself does not prevent acceptance of incorrect transitions, which requires a careful validation procedure).

To describe the vibrational quantum states of CO<sub>2</sub>, we have adopted the AFGL (Air Force Geophysics Laboratory) notation [50–52]. This system avoids super- and subscripts, making it especially suitable for electronic databases. Thus, the vibrational states are represented by the quantum numbers  $v_1$  (symmetric stretch),  $v_2$  and  $l_2$  (representing a doubly degenerate bend), and  $v_3$  (antisymmetric stretch). Additionally, a ranking index  $r$  helps to account for Fermi resonances, which complicate considerably the interpretation of the rovibrational spectra of CO<sub>2</sub> [50]. The index  $r$  ranges from 1 to  $v_1 + 1$  [52–54].

Unlike for most small molecules, for CO<sub>2</sub> there have been multiple choices for  $P$ , the polyad number, which is the sum of quantum numbers multiplied by specific weights, helping to describe the structure of the vibrational states [55–58]. In this study, following AFGL, we use the expression  $P = 2v_1 + v_2 + 3v_3$ . To fully describe the rovibrational states of CO<sub>2</sub>, two more descriptors are required,  $J$ , the rotational quantum number (an exact quantum number), and  $p$ , representing rotationless parity, labeled as ‘ $e$ ’ or ‘ $f$ ’.

Thus, the full label for a rovibrational quantum state is written as  $(J v_1 v_2 l_2 v_3 r p)$ , and the same descriptors have been applied to all twelve isotopologues of carbon dioxide. A key rule in AFGL notation is that  $v_2$  and  $l_2$  are always equal. Unlike the standard (Herzberg) notation, which can cause shifts in energy level ordering across isotopologues, the AFGL notation maintains a consistent structure, though it introduces an extra descriptor.

There are several additional points to note about the descriptors used; these translate to rules which are especially useful to check the transitions found in the literature. First, non-degenerate states, where  $v_2 = l_2 = 0$ , always have parity ‘ $e$ ’; thus, some sources even omit this parity label. Second, states with  $l_2 > 0$  have both ‘ $e$ ’ and ‘ $f$ ’ parity states for each  $J$ . Third,  $J$  must be at least as large as  $l_2$ , meaning vibrational states with  $l_2 > 0$  do not have a  $J = 0$  level.

## 2.3. Selection rules

For all asymmetric CO<sub>2</sub> isotopologues, the equilibrium geometry belongs to the  $C_{\infty v}$  point group, which means that there are no formal selection rules on vibrational transitions. The rotational state selection rules for one-photon dipole-allowed transitions are  $\Delta J = 0, \pm 1$ , and when

$$\Delta J = 0; \quad e \leftrightarrow f, \quad (1)$$

meaning that the rotationless parity changes between the initial and the final states in the Q branch, whereas when

$$\Delta J = \pm 1; \quad e \leftrightarrow e, \quad f \leftrightarrow f, \quad (2)$$

indicating no rotationless parity change in the P and R branches.

Unlike for the symmetric 626 isotopologue, where all nuclear spins are zero and half the levels are missing due to the Pauli principle, all levels are allowed for both 737 and 738. In particular, 737, as a symmetric molecule, has constraints placed on it by the Pauli principle, leading to distinct *ortho* and *para* components in its spectroscopic network, which have to be linked using a theoretically-determined “magic number” which gives the energy difference of the roots of the *ortho* and *para* principal components. Because <sup>17</sup>O has nuclear spin  $I = 5/2$  (i.e., greater than zero), there are *ortho* levels when  $(J + v_3 + \ell_2 + p)$  is odd, with a weight of 21, and *para* levels when  $(J + v_3 + \ell_2 + p)$  is even, with a weight of 15 (or a 7:5 weighting). In these expressions  $p = 0$  for  $e$  rotationless parity states and 1 for  $f$  rotationless parity with total parity given by  $(-1)^{J+p}$ .

## 3. Experimental studies of line positions

For 738/737, a total of 2058/1831 transitions were collected from 10/5 sources. Table 3 summarizes the most relevant characteristics of these sources. The wavenumber range covered is 624–7888 cm<sup>-1</sup> for 738 and 624–6739 cm<sup>-1</sup> for 737. Among all the measured transitions, only 1488 and 1349 are unique for 738 and 737, respectively. All of the collected transitions are available in the Supplementary Material in the input files “transitions\_738.txt”/“transitions\_737.txt”; these are the files used during the MARVEL analysis. In these files, each transition is characterized by (a) a line position (in units that are indicated in the segment file), (b) an initial and an adjusted, expanded (two-sigma) uncertainty for the line position (the adjusted uncertainty is the one which ensures that the final set of input transitions is self-consistent), (c) the rovibrational assignments of the upper and lower states (see Section 2.2 for a description of the labels of the quantum states and Section 2.3 for the selection rules), and (d) a line tag, a metadata string providing a unique identifier (for multi-author publications, each tag contains the last two digits of the year of the publication and the first two characters of the last names of the authors, up to the first four authors) plus a sequence number for each line.

The spectroscopic network of 738 has two large components, one with 430 and another with 495 energy levels. Although 738 is asymmetric, these two SNs correspond to what would be *para* and *ortho* sets in 737, showing that for 738 breaking the symmetry leads to new transitions that are too weak to have been observed up until now. To connect the large two components we use the CDSD-296 energy value, 0.713887  $hc$  cm<sup>-1</sup>, for the  $J = 1$  level with an estimated expanded uncertainty of  $5 \times 10^{-6} hc$  cm<sup>-1</sup>. The expanded SN of 738 contains two smaller floating components, as well, both with 10 energy levels. We added two further artificial transitions, with an expanded uncertainty of 0.005 cm<sup>-1</sup>, using rotational energy values from the CDSD-296 database to link these smaller floating components to the unified principal component of 738. In the transitions file, these artificial transitions are tagged as ‘19CDSD’.

The spectroscopic network of the experimentally measured transitions of <sup>17</sup>O<sup>13</sup>C<sup>17</sup>O is made up of several components. The largest components contain 320, 319, 82, 80, 17, 16, and 15 rovibrational

**Table 3**

$^{17}\text{O}^{13}\text{C}^{18}\text{O}$  (738) and  $^{17}\text{O}^{13}\text{C}^{17}\text{O}$  (737) data sources used in this work and their characteristics, including the number of measured ( $A$ ), floating ( $F$ ), validated ( $V$ ), and deleted ( $D$ ) transitions, while  $U^{\text{CS}}$  is the average expanded ‘claimed source’ uncertainty, and  $U^{\text{MS}}$  is the average expanded ‘MARVEL-suggested source’ uncertainty of the transitions of the given source.

Isotopologue	Source	Range/ $\text{cm}^{-1}$	$A/F/V/D$	$U^{\text{CS}}/\text{cm}^{-1}$	$U^{\text{MS}}/\text{cm}^{-1}$
$^{17}\text{O}^{13}\text{C}^{18}\text{O}$ (738)	98TeClVa [25]	623.64–2285.13	89/0/89/0	$2.5 \times 10^{-4}$	$3.1 \times 10^{-4}$
	12LyKaJaLu [18]	2181.99–4798.25	727/82/645/0	$1.1 \times 10^{-3}$	$1.2 \times 10^{-3}$
	14BoJaLyTa [19]	3390.63–4681.03	557/83/474/0	$2.1 \times 10^{-4}$	$2.0 \times 10^{-4}$
	15BoJaLyTa [21]	4738.98–4911.67	99/0/99/0	$4.1 \times 10^{-4}$	$7.1 \times 10^{-4}$
	19MoKaPeTa [24]	5748.47–5850.02	53/0/53/0	$1.0 \times 10^{-3}$	$1.0 \times 10^{-3}$
	18KaCeMoKa [23]	5796.99–5851.32	20/0/20/0	$1.0 \times 10^{-3}$	$1.0 \times 10^{-3}$
	14KaCaMoKa [20]	5934.73–6714.19	273/3/270/0	$1.0 \times 10^{-3}$	$1.2 \times 10^{-3}$
	08PePeCa [16]	5946.42–6714.19	130/0/130/0	$1.0 \times 10^{-3}$	$1.2 \times 10^{-3}$
	17KaCaKaTa [22]	7815.54–7887.65	77/0/77/0	$1.0 \times 10^{-3}$	$1.1 \times 10^{-3}$
	10CaSoMoPe [17]	7837.44–7886.66	30/0/30/0	$8.0 \times 10^{-4}$	$1.1 \times 10^{-3}$
$^{17}\text{O}^{13}\text{C}^{17}\text{O}$ (737)	98TeClVa [25]	624.16–2292.55	90/1/89/0	$2.5 \times 10^{-4}$	$2.5 \times 10^{-4}$
	12LyKaJaLu [18]	1967.02–6739.01	952/122/830/0	$1.1 \times 10^{-3}$	$1.1 \times 10^{-3}$
	14BoJaLyTa [19]	3406.30–4681.17	579/98/481/0	$1.6 \times 10^{-4}$	$1.4 \times 10^{-4}$
	15BoJaLyTa [21]	4681.93–4946.62	169/0/169/0	$1.0 \times 10^{-3}$	$1.2 \times 10^{-3}$
	19MoKaPeTa [24]	5780.08–5849.18	26/1/25/0	$1.0 \times 10^{-3}$	$1.0 \times 10^{-3}$

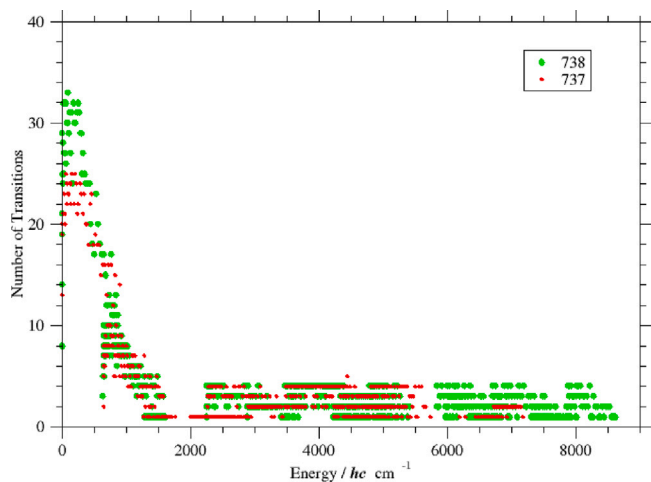


Fig. 1. The number of transitions incident to each energy level as a function of the empirical rovibrational energy determined in this study for  $^{17}\text{O}^{13}\text{C}^{18}\text{O}$  (738, green dots) and  $^{17}\text{O}^{13}\text{C}^{17}\text{O}$  (737, red dots).

energy levels. The first two energy sets form the *ortho* and *para* principal components of the spectroscopic network. To connect them, we use what we call a ‘magic number’, corresponding to an artificial transition that connects the lowest energy levels of the *ortho* and *para* principal components. In other words, our aim is to know the absolute value of the lowest energy level of the *ortho* principal component (that of the *para* principal component is set to zero with zero uncertainty by definition). This value,  $0.734423 \text{ hc cm}^{-1}$ , is taken from CDSD-296 [43]. Our previous experience [38] suggests that the deviation of this MARVEL energy from the CDSD-296 result is on the order of  $10^{-6} \text{ hc cm}^{-1}$ ; thus, the uncertainty of this magic number is set to  $5 \times 10^{-6} \text{ hc cm}^{-1}$ . To link the larger floating components to the *ortho* and *para* principal components, we chose 14 artificial transitions, with an expanded uncertainty of  $0.005 \text{ cm}^{-1}$ , using rotational energy values from the CDSD-296 database. In the transition file, these artificial transitions are tagged as ‘19CDS’.

## 4. Results and discussion

### 4.1. Energy levels

Using the MARVEL procedure, 945/877 empirical rovibrational energy levels are determined by 2058(1488)/1831(1349) measured

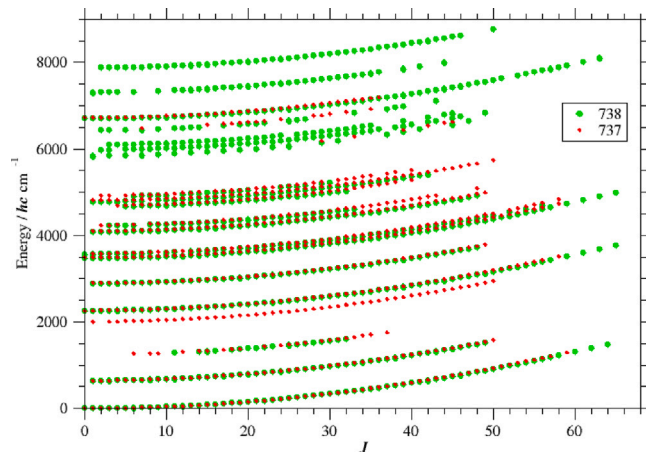


Fig. 2. Energy levels determined using MARVEL as function of the rotational quantum number  $J$  for  $^{17}\text{O}^{13}\text{C}^{18}\text{O}$  (738, green dots) and  $^{17}\text{O}^{13}\text{C}^{17}\text{O}$  (737, red dots).

(unique) observed transitions for 738/737, respectively. All these energy levels are available in the files ‘Energylevels\_738.txt’ and ‘Energylevels\_737.txt’ of the Supplementary Material. Each energy level of these data files is characterized by (a) a rovibrational label, (b) an empirical (MARVEL) energy (in  $\text{hc cm}^{-1}$ ), (c) an expanded (two-sigma) energy uncertainty (in  $\text{hc cm}^{-1}$ ), and (d) the number of transitions incident to this state.

Fig. 1 shows the number of transitions incident to each energy level and their distribution as a function of energy. This figure confirms that the degree distribution of the nodes of spectroscopic networks formed by experimentally measured transitions appears to be heavy tailed [59].

The empirical rovibrational energy levels determined in this study have  $J$  values up to 65 for 738 and up to 59 for 737, as seen in Fig. 2. Each dotted curve in Fig. 2 corresponds to a vibrational band, with the dots representing different  $J$  values. The stacks of energy levels clearly show the semirigid character of the  $\text{CO}_2$  molecule and that there are missing empirical energy levels even for low  $J$  values.

Fig. 3 shows the polyad numbers,  $P = 2v_1 + v_2 + 3v_3$ , of the empirical rovibrational energy levels as a function of their energy. The  $P$  values range from 0 to 11 for 738 and from 0 to 10 for 737. Note the nearly linear, stepwise increase of  $P$  with the increase of the energy values and the significant overlaps in the energies. Fig. 3 also illustrates the distribution of the derived energy levels over Fermi resonances as characterized by the resonance number  $r$ .

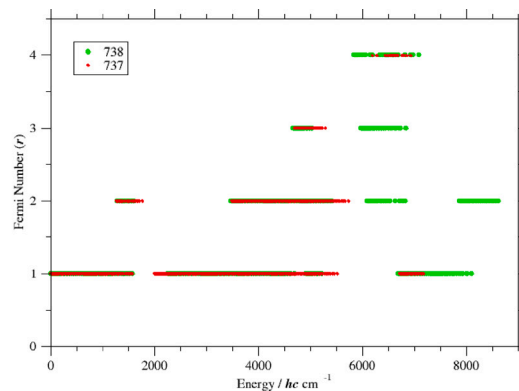
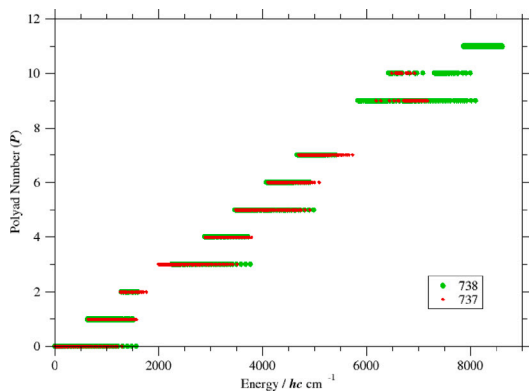


Fig. 3. Polyad number,  $P = 2v_1 + v_2 + 3v_3$ , (left panel) and Fermi number  $r$  for each rovibrational energy level determined in this study, using MARVEL, for  $^{17}\text{O}^{13}\text{C}^{18}\text{O}$  (738) and  $^{17}\text{O}^{13}\text{C}^{17}\text{O}$  (737).

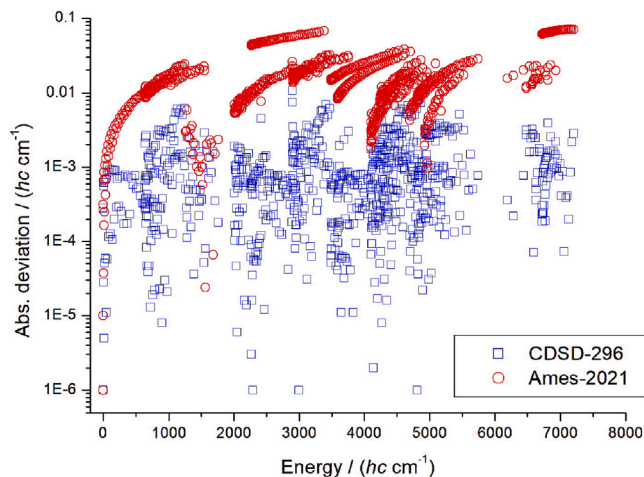


Fig. 4. Comparison between the empirical rovibrational energies of the present  $^{17}\text{O}^{13}\text{C}^{18}\text{O}$  dataset with those of CDS-296 [43] (blue squares) and Ames-2021 [34] (red circles).

#### 4.2. Comparison with the CDS-296 and Ames-2021 databases

We have made detailed comparisons of the empirical rovibrational energy levels determined in this study with their counterpart in the CDS-296 [43] and Ames-2021 [34] datasets by matching the quantum numbers of individual levels. Fig. 4 shows the absolute deviations of the rovibrational energy levels of  $^{17}\text{O}^{13}\text{C}^{18}\text{O}$  between the MARVEL and the CDS-296 [43] and Ames-2021 [34] datasets. The root-mean-square deviations of the present MARVEL and the CDS-296 and AMES-2021 energies are 0.0020 and 0.0379  $hc\text{ cm}^{-1}$ , respectively. We found only one transition whose wavenumber value differs from the CDS-296 result by more than 0.01  $\text{cm}^{-1}$ . This is the (49 3 0 0 1 3 e)  $\leftarrow$  (48 0 0 0 0 1 e) transition reported by 14KaCaMoKa [20]: its experimentally measured wavenumber is 6002.2253(10)  $\text{cm}^{-1}$ , while its CDS-296 line position is 6002.212631  $\text{cm}^{-1}$ . Since this transition is the only one that determines the value of (49 3 0 0 1 3 e) energy levels, we cannot determine whether the experimental or the CDS-296 line position is correct.

Fig. 5 is similar to Fig. 4, it shows the absolute deviations of the rovibrational energy levels of  $^{17}\text{O}^{13}\text{C}^{17}\text{O}$  between the MARVEL and the CDS-296 and Ames-2021 datasets. The root-mean-square deviations of the present MARVEL and the CDS-296 and AMES-2021 energies are 0.0020 and 0.0242  $hc\text{ cm}^{-1}$ , respectively. It can also be seen from Fig. 5 that there is no MARVEL energy level that differs from its CDS-296 counterpart by more than 0.01  $hc\text{ cm}^{-1}$ .

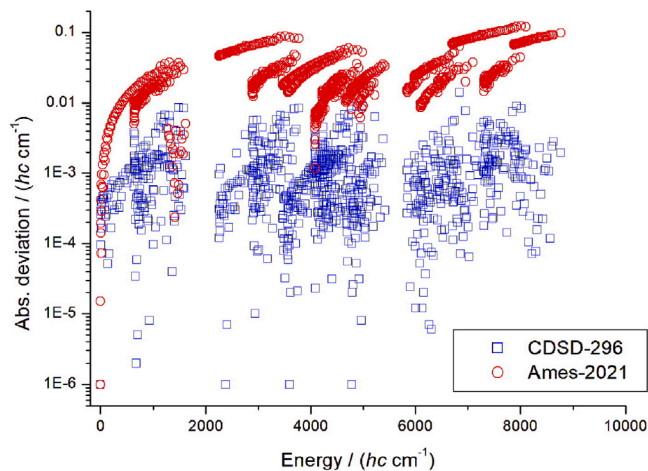


Fig. 5. Comparison between the empirical rovibrational energies of the present  $^{17}\text{O}^{13}\text{C}^{17}\text{O}$  dataset with those of CDS-296 [43] (blue squares) and Ames-2021 [34] (red circles).

#### 5. Summary and conclusions

This study presented a comprehensive analysis of all the available high-resolution, rovibrational transitions of the eleventh and twelfth most abundant, triply substituted isotopologues of carbon dioxide,  $^{17}\text{O}^{13}\text{C}^{18}\text{O}$  and  $^{17}\text{O}^{13}\text{C}^{17}\text{O}$ . For this analysis, the MARVEL algorithm and code [26–28,44] were employed. The transitions forming the basis of the MARVEL analysis were the 2058/1831 measured transitions collected from 10/5 literature sources for the 738/737 isotopologues.

The transitions collected cover the wavenumber range of 624–7888  $hc\text{ cm}^{-1}$  for 738, and 624–6739  $hc\text{ cm}^{-1}$  for 737. The number of unique transitions this datasets contain is 1488/1349 for 738/737. None of the transitions collected had to be excluded from our final analysis. As a result, 945/877 empirical rovibrational energy levels, extending up to 8762  $hc\text{ cm}^{-1}$  for 738 and up to 7201  $hc\text{ cm}^{-1}$  for 737, were determined. The average expanded uncertainty of the levels is  $9 \times 10^{-4} hc\text{ cm}^{-1}$  for 738, and  $2 \times 10^{-3} hc\text{ cm}^{-1}$  for 737.

Comparisons with this and our previous studies of  $\text{CO}_2$  isotopologues with datasets provided by NASA Ames and CDS-296, see Table 2, show that for the twelve stable  $\text{CO}_2$  isotopologues, agreement with the CDS-296 data is significantly better, by more than an order of magnitude on average for the absolute deviation. While the CDS-296 results are based on isotopologue-specific effective Hamiltonian fits to the experimental results, the NASA Ames calculations are performed using a single potential energy surface tuned to reproduce these results. The NASA Ames procedure therefore implicitly assumes the validity of

the Born–Oppenheimer approximation; the variation of the differences between our MARVEL energy levels and these results therefore gives an indication about the accuracy of this fundamental approximation of quantum chemistry. It is our intention to use the complete set of empirical energy levels derived by our MARVEL studies on the twelve stable isotopologues of CO<sub>2</sub> as a starting point to try and model effects beyond the Born–Oppenheimer approximation in molecules which do not contain hydrogen.

### CRedit authorship contribution statement

**Ala'a A.A. Azzam:** Writing – original draft, Supervision, Formal analysis, Data curation, Conceptualization. **Joud M.A. AlAlawin:** Investigation, Data curation. **Jonathan Tennyson:** Writing – review & editing, Project administration, Funding acquisition, Conceptualization. **Tibor Furtenbacher:** Software, Methodology, Data curation, Investigation, Formal analysis. **Attila G. Császár:** Writing – review & editing, Methodology, Funding acquisition, Conceptualization.

### Declaration of competing interest

The authors declare no conflict of interest.

### Acknowledgments

The UK and Jordanian co-authors thank STFC, United Kingdom for funding the UK–Jordan collaboration under the Newton Fund grant ST/T001429/1. J.T. acknowledges the support of the European Research Council (ERC) under the European Union's Horizon 2020 research and innovation programme through Advance Grant number 883830. The work of A.G.C. and F.T. received support from the National Research, Development and Innovation Office of Hungary (NK-FIH, grant number K138233).

### Appendix A. Supplementary data

Supplementary material related to this article can be found online at <https://doi.org/10.1016/j.jqsrt.2025.109485>.

### Data availability

The MARVEL input file, including all the transitions, and the MARVEL output file, with all the energy levels, are supplied as Supplementary Material to this paper. Both the measured transitions and the empirical energy levels have expanded (two-sigma) uncertainties attached to them.

### References

- Bernath PF, McElroy CT, Abrams MC, Boone CD, Butler M, Camy-Peyret C, Carleer M, Clerbaux C, Coheur P, Colin R, DeCola P, DeMazière M, Drummond JR, Dufour D, Evans WFJ, Fast H, Fussen D, Gilbert K, Jennings DE, Llewellyn EJ, Lowe RP, Mahieu E, McConnell JC, McHugh M, McLeod SD, Michaud R, Midwinter C, Nassar R, Nichitief F, Nowlan C, Rinsland CP, Rochon YJ, Rowlands N, Semeniuk K, Simon P, Skelton R, Sloan JJ, Soucy M, Strong K, Tremblay P, Turnbull D, Walker KA, Walkty I, Wardle DA, Wehrle V, Zander R, Zou J. Atmospheric chemistry experiment (ACE): Mission overview. *Geophys Res Lett* 2005;32. <http://dx.doi.org/10.1029/2005gl022386>.
- Butz A, Guerlet S, Hasekamp O, Schepers D, Galli A, Aben I, Frankenberg C, Hartmann J-M, Tran H, Kuze A, Keppel-Aleks G, Toon G, Wunch D, Wennberg P, Deutscher N, Griffith D, Macatangay R, Messerschmidt J, Notholt J, Warneke T. Toward accurate CO<sub>2</sub> and CH<sub>4</sub> observations from GOSAT. *Geophys Res Lett* 2011;38. <http://dx.doi.org/10.1029/2011gl047888>.
- Eldering A, Taylor TE, O'Dell CW, Pavlick R. The OCO-3 mission: measurement objectives and expected performance based on 1 year of simulated data. *Atmos Meas Tech* 2019;12:2341–70. <http://dx.doi.org/10.5194/amt-12-2341-2019>.
- Hobbs JM, Drouin BJ, Oyafuso F, Payne VH, Gunson MR, McDuffie J, Mlawer EJ. Spectroscopic uncertainty impacts on OCO-2/3 retrievals of XCO<sub>2</sub>. *J Quant Spectrosc Radiat Transfer* 2020;257:107360. <http://dx.doi.org/10.1016/j.jqsrt.2020.107360>.
- Thorpe AK, Green RO, Thompson DR, Brodrick PG, Chapman JW, Elder CD, Irakulis-Loitxate I, Cusworth DH, Ayasse AK, Duren RM, Frankenberg C, Guanter L, Worden JR, Dennison PE, Roberts DA, Chadwick KD, Eastwood ML, Fahlen JE, Miller CE. Attribution of individual methane and carbon dioxide emission sources using EMIT observations from space. *Sci Adv* 2023;9:eadh2391. <http://dx.doi.org/10.1126/sciadv.adh2391>.
- Ward JK, Strain BR. Elevated CO<sub>2</sub> studies: past, present and future. *Tree Physiol* 1999;19:211–20. <http://dx.doi.org/10.1093/treephys/19.4.5.211>.
- Pearson PN, Palmer MR. Atmospheric carbon dioxide concentrations over the past 60 million years. *Nature* 2000;406:695–9. <http://dx.doi.org/10.1038/35021000>.
- Romps DM, Seeley JT, Edman JP. Why the forcing from carbon dioxide scales as the logarithm of its concentration. *J Clim* 2022;35:4027–47. <http://dx.doi.org/10.1175/JCLI-D-21-0275.1>.
- Shine KP, Perry GE. Radiative forcing due to carbon dioxide decomposed into its component vibrational bands. *Q J R Meteorol* 2023;149(754):1856–66. <http://dx.doi.org/10.1002/qj.4485>.
- Calvin K, Dasgupta D, Krinner G, Mukherji A, Thorne PW, Trisos C, Romero J, Aldunce P, Barrett K, Blanco G, Cheung WWL, Connors S, Denton F, Diongue-Niang A, Dodman D, Garschagen M, Geden O, Hayward B, Jones C, Jotzo F, Krug T, Lasco R, Lee Y-Y, Masson-Delmotte V, Meinshausen M, Mintenbeck K, Mokssit A, Otto FEL, Pathak M, Pirani A, Poloczanska E, Pörtner H-O, Revi A, Roberts DC, Roy J, Ruane AC, Skea J, Shukla PR, Slade R, Slangen A, Sokona Y, Sörensson AA, Tignor M, van Vuuren D, Wei Y-M, Winkler H, Zhai P, Zommers Z, Hourcade J-C, Johnson FX, Pachauri S, Simpson NP, Singh C, Thomas A, Totin E, Alegría A, Armour K, Bednar-Friedl B, Blok K, Cissé G, Dentener F, Eriksen S, Fischer E, Garner G, Guivarch C, Haasnoot M, Hansen G, Hauser M, Hawkins E, Hermans T, Kopp R, Leprince-Ringuet N, Lewis J, Ley D, Ludden C, Niamir L, Nicholls Z, Some S, Szopa S, Trewin B, van der Wijst K-I, Winter G, Witting M, Birt A, Ha M. IPCC, 2023: climate change 2023: synthesis report. contribution of working groups I, II and III to the sixth assessment report of the intergovernmental panel on climate change [core writing team, H. Lee and J. Romero (eds.)]. Tech. rep., Geneva, Switzerland: IPCC; 2023.
- Noel S, Buchwitz M, Hilker M, Reuter M, Weimer M, Bovensmann H, Burrows JP, Boesch H, Lang R. Greenhouse gas retrievals for the CO2M mission using the FOCAL method: first performance estimates. *Atmos Meas Tech* 2024;17:2317–34. <http://dx.doi.org/10.5194/amt-17-2317-2024>.
- Laughner JL, Toon GC, Mendonca J, Petri C, Roche S, Wunch D, Blavier J-F, Griffith DWT, Heikkinen P, Keeling RF, Kiel M, Kivi R, Roehl CM, Stephens BB, Baier BC, Chen H, Choi Y, Deutscher NM, DiGangi JP, Gross J, Herkommer B, Jeseck P, Laemmel T, Lan X, McGee E, McKain K, Miller J, Morino I, Notholt J, Ohyama H, Pollard DF, Rettinger M, Riris H, Rousogonous C, Sha MK, Shiomi K, Strong K, Sussmann R, Te Y, Velazco VA, Wofsy SC, Zhou M, Wennberg PO. The total carbon column observing network's GGG2020 data version. *Earth Syst Sci Data* 2024;16:2197–260. <http://dx.doi.org/10.5194/essd-16-2197-2024>.
- Gordon IE, Rothman LS, Hargreaves RJ, Hashemi R, Karlovets EV, Skinner FM, Conway EK, Hill C, Kochanov RV, Tan Y, Wcislo P, Finenko AA, Nelson K, Bernath PF, Birk M, Boudon V, Campargue A, Chance KV, Coustenis A, Drouin BJ, Flaud J, Gamache RR, Hodges JT, Jacquemart D, Mlawer EJ, Nikitin AV, Perevalov VI, Rotger M, Tennyson J, Toon GC, Tran H, Tyuterev VG, Adkins EM, Baker A, Barbe A, Cané E, Császár AG, Dudaryonok A, Egorov O, Fleisher AJ, Fleurbaey H, Foltynowicz A, Furtenbacher T, Harrison JJ, Hartmann J, Horneman V, Huang X, Karman T, Karns J, Kassi S, Kleiner I, Kofman V, Kwabia-Tchana F, Lavrentieva NN, Lee TJ, Long DA, Lukashevskaya AA, Lyulin OM, Makhnev VY, Matt W, Massie ST, Melosso M, Mikhailenko SN, Mondelain D, Müller HSP, Naumenko OV, Perrin A, Polyansky OL, Raddaoui E, Raston PL, Reed ZD, Rey M, Richard C, Tóbiás R, Sadiek I, Schwenke DW, Starikova E, Sung K, Tamassia F, Tashkun SA, Vander Auwera J, Vasilenko IA, Vigasin AA, Villanueva GL, Vispoel B, Wagner G, Yachmenev A, Yurchenko SN. The HITRAN2020 molecular spectroscopic database. *J Quant Spectrosc Radiat Transfer* 2022;277:107949. <http://dx.doi.org/10.1016/j.jqsrt.2021.107949>.
- Shine KP, Perry GE. Radiative forcing due to carbon dioxide decomposed into its component vibrational bands. *Q J R Meteorol* 2023;149:1856–66. <http://dx.doi.org/10.1002/qj.4485>.
- Shine KP, Perry GE. Radiative forcing due to carbon dioxide decomposed into its component vibrational bands. *Q J R Meteorol Soc* 2023;149(754):1856–66. <http://dx.doi.org/10.1002/qj.4485>. URL <https://rmets.onlinelibrary.wiley.com/doi/pdf/10.1002/qj.4485>. URL <https://rmets.onlinelibrary.wiley.com/doi/abs/10.1002/qj.4485>.
- Perevalov BV, Perevalov VI, Campargue A. A (nearly) complete experimental line list for <sup>13</sup>C<sup>16</sup>O<sub>2</sub>, <sup>16</sup>O<sup>13</sup>C<sup>18</sup>O, <sup>16</sup>O<sup>13</sup>C<sup>17</sup>O, <sup>13</sup>C<sup>18</sup>O<sub>2</sub> and <sup>17</sup>O<sup>13</sup>C<sup>18</sup>O by high-sensitivity CW-CRDS spectroscopy between 5851 and 7045 cm<sup>-1</sup>. *J Quant Spectrosc Radiat Transfer* 2008;109:2437–62. <http://dx.doi.org/10.1016/j.jqsrt.2008.03.010>.
- Campargue A, Song KF, Mouton N, Perevalov VI, Kassi S. High sensitivity CW-cavity ring down spectroscopy of five <sup>13</sup>CO<sub>2</sub> isotopologues of carbon dioxide in the 1.26–1.44 μm region (i): Line positions. *J Quant Spectrosc Radiat Transfer* 2010;111:659–74. <http://dx.doi.org/10.1016/j.jqsrt.2009.11.013>.

- [18] Lyulin OM, Karlovets EV, Jacquemart D, Lu Y, Liu AW, Perevalov VI. Infrared spectroscopy of  $^{17}\text{O}$ - and  $^{18}\text{O}$ -enriched carbon dioxide in the 1700–8300  $\text{cm}^{-1}$  wavenumber region. *J Quant Spectrosc Radiat Transfer* 2012;113:2167–81. <http://dx.doi.org/10.1016/j.jqsrt.2012.06.028>.
- [19] Borkov YG, Jacquemart D, Lyulin OM, Tashkun SA, Perevalov VI. Infrared spectroscopy of  $^{17}\text{O}$ - and  $^{18}\text{O}$ -enriched carbon dioxide: Line positions and intensities in the 3200–4700  $\text{cm}^{-1}$  region. Global modeling of the line positions of  $^{16}\text{O}^{12}\text{C}^{17}\text{O}$  and  $^{17}\text{O}^{12}\text{C}^{17}\text{O}$ . *J Quant Spectrosc Radiat Transfer* 2014;137:57–76. <http://dx.doi.org/10.1016/j.jqsrt.2013.11.008>.
- [20] Karlovets EV, Campargue A, Mondelain D, Kassi S, Tashkun SA, Perevalov VI. High sensitivity cavity ring down spectroscopy of  $^{18}\text{O}$  enriched carbon dioxide between 5850 and 7000  $\text{cm}^{-1}$ : Part II. Analysis and theoretical modeling of the  $^{12}\text{C}^{18}\text{O}_2$ ,  $^{13}\text{C}^{18}\text{O}_2$  and  $^{16}\text{O}^{13}\text{C}^{18}\text{O}$  spectra. *J Quant Spectrosc Radiat Transfer* 2014;136:71–88. <http://dx.doi.org/10.1016/j.jqsrt.2013.11.005>.
- [21] Borkov YG, Jacquemart D, Lyulin OM, Tashkun SA, Perevalov VI. Infrared spectroscopy of  $^{17}\text{O}$ - and  $^{18}\text{O}$ -enriched carbon dioxide: Line positions and intensities in the 4681–5337  $\text{cm}^{-1}$  region. *J Quant Spectrosc Radiat Transfer* 2015;159:1–10. <http://dx.doi.org/10.1016/j.jqsrt.2015.02.019>.
- [22] Karlovets E, Campargue A, Kassi S, Tashkun S, Perevalov V. Analysis and theoretical modeling of  $^{18}\text{O}$  enriched carbon dioxide spectrum by CRDS near 1.35  $\mu\text{m}$ : (II)  $^{16}\text{O}^{13}\text{C}^{18}\text{O}$ ,  $^{16}\text{O}^{13}\text{C}^{17}\text{O}$ ,  $^{12}\text{C}^{18}\text{O}_2$ ,  $^{17}\text{O}^{12}\text{C}^{18}\text{O}$ ,  $^{12}\text{C}^{17}\text{O}_2$ ,  $^{13}\text{C}^{18}\text{O}_2$  and  $^{17}\text{O}^{13}\text{C}^{18}\text{O}$ . *J Quant Spectrosc Radiat Transfer* 2017;191:75–87. <http://dx.doi.org/10.1016/j.jqsrt.2017.01.038>.
- [23] Karlovets EV, Čermák P, Mondelain D, Kassi S, Campargue A, Tashkun SA, Perevalov VI. Analysis and theoretical modeling of the  $^{18}\text{O}$  enriched carbon dioxide spectrum by CRDS near 1.74  $\mu\text{m}$ . *J Quant Spectrosc Radiat Transfer* 2018;217:73–85. <http://dx.doi.org/10.1016/j.jqsrt.2018.05.017>.
- [24] Mondelain D, Karlovets E, Perevalov V, Tashkun S, Campargue A. High-sensitivity CRDS absorption spectrum of  $^{17}\text{O}$  enriched carbon dioxide near 1.74  $\mu\text{m}$ . *J Mol Spectrosc* 2019;362:84–9. <http://dx.doi.org/10.1016/j.jms.2019.06.004>.
- [25] Teffo J-L, Claveau C, Valentin A. Infrared fundamental bands of  $\text{O}^{13}\text{C}^{17}\text{O}$  isotopic variants of carbon dioxide. *J Quant Spectrosc Radiat Transfer* 1998;59:151–64. [http://dx.doi.org/10.1016/S0022-4073\(97\)00109-X](http://dx.doi.org/10.1016/S0022-4073(97)00109-X).
- [26] Császár AG, Czakó G, Furtenbacher T, Mátys E. An active database approach to complete rotational–vibrational spectra of small molecules. *Annu Rep Comput Chem* 2007;3:155–76. [http://dx.doi.org/10.1016/S1574-1400\(07\)03009-5](http://dx.doi.org/10.1016/S1574-1400(07)03009-5).
- [27] Furtenbacher T, Császár AG, Tennyson J. MARVEL: measured active rotational–vibrational energy levels. *J Mol Spectrosc* 2007;245:115–25. <http://dx.doi.org/10.1016/j.jms.2007.07.005>.
- [28] Furtenbacher T, Császár AG. MARVEL: measured active rotational–vibrational energy levels. II. Algorithmic improvements. *J Quant Spectrosc Radiat Transfer* 2012;113:929–35. <http://dx.doi.org/10.1016/j.jqsrt.2012.01.005>.
- [29] Császár AG, Furtenbacher T, Árendás P. Small molecules – big data. *J Phys Chem A* 2016;120:8949–69. <http://dx.doi.org/10.1021/acs.jpca.6b02293>.
- [30] Tóbiás R, Furtenbacher T, Tennyson J, Császár AG. Accurate empirical rovibrational energies and transitions of  $\text{H}_2^{16}\text{O}$ . *Phys Chem Chem Phys* 2019;21:3473–95. <http://dx.doi.org/10.1039/c8cp05169k>.
- [31] Császár AG, Furtenbacher T. Spectroscopic networks. *J Mol Spectrosc* 2011;266:99–103. <http://dx.doi.org/10.1016/j.jms.2011.03.031>.
- [32] Furtenbacher T, Császár AG. The role of intensities in determining characteristics of spectroscopic networks. *J Mol Struct* 2012;1009:123–9. <http://dx.doi.org/10.1016/j.molstruc.2011.10.057>.
- [33] Huang X, Schwenke DW, Lee TJ. Isotopologue consistency of semi-empirically computed infrared line lists and further improvement for rare isotopologues:  $\text{CO}_2$  and  $\text{SO}_2$  case studies. *J Quant Spectrosc Radiat Transfer* 2019;230:222–46. <http://dx.doi.org/10.1016/j.jqsrt.2019.03.002>.
- [34] Huang X, Schwenke DW, Freedman RS, Lee TJ.  $\text{CO}_2$  dipole moment surface and IR line lists: Toward 0.1% uncertainty for  $\text{CO}_2$  IR intensities. *Ames- J Phys Chem A* 2021;126(35):5940–64. <http://dx.doi.org/10.1021/acs.jpca.2c01291>, PMID: 36007245.
- [35] Tennyson J, Yurchenko SN, Zhang J, Bowesman CA, Brady RP, Buldyreva J, Chubb KL, Gamache RR, Gorman MN, Guest ER, Hill C, Kefala K, Lynas-Gray AE, Mellor TM, McKemmish LK, Mitev GB, Mizus II, Owens A, Peng Z, Perri AN, Pezzella M, Polyansky OL, Qu Q, Semenov M, Smola O, Solokov A, Somogyi W, Upadhyay A, Wright SOM, Zobov NF. Release of the ExoMol database: molecular line lists for exoplanet and other hot atmospheres. *J Quant Spectrosc Radiat Transf* 2024;326:109083. <http://dx.doi.org/10.1016/j.jqsrt.2024.109083>.
- [36] Azzam AAA, Alatoom D, Abou Doud BMJ, Abu Shersheer MQA, Almasri BKM, Bader CNM, Musleh BOAK, Obaido MJZ, Abu Khudair AMH, Al Shatarat AWM, Qattan BIM, Hamamsy LHM, Saafneh AOG, Also'ub MNA, Alkhashashneh MMA, Al-Zawahra HOM, Ibrahim MTI, Tennyson J, Yurchenko SN, Furtenbacher T, Császár AG. The 626m24 dataset of validated transitions and empirical rovibrational energy levels of  $^{16}\text{O}^{12}\text{C}^{16}\text{O}$ . *Sci Data* 2025;12:532. <http://dx.doi.org/10.1038/s41597-025-04755-w>.
- [37] Ibrahim MTI, Alatoom D, Furtenbacher T, Császár AG, Yurchenko SN, Azzam AAA, Tennyson J. MARVEL analysis of high-resolution rovibrational spectra of  $^{13}\text{C}^{16}\text{O}_2$ . *J Comput Chem* 2024;45:969–84. <http://dx.doi.org/10.1002/jcc.27266>.
- [38] Alatoom D, Ibrahim MTI, Furtenbacher T, Császár AG, Alghizzawi M, Yurchenko SN, Azzam AAA, Tennyson J. MARVEL analysis of high-resolution rovibrational spectra of  $^{16}\text{O}^{12}\text{C}^{18}\text{O}$ . *J Comput Chem* 2024;45:2558. <http://dx.doi.org/10.1002/jcc.27453>.
- [39] Obaidat SA, Azzam AA, Alatoom D, Ibrahim MTI, Tennyson J, Furtenbacher T, Császár AG. Marvel analysis of high-resolution rovibrational spectra of  $^{16}\text{O}^{12}\text{C}^{17}\text{O}$ . *J Quant Spectrosc Radiat Transfer* 2025;340:109444. <http://dx.doi.org/10.1016/j.jqsrt.2025.109444>, URL <https://www.sciencedirect.com/science/article/pii/S0022407325001062>.
- [40] Azzam AAA, Tennyson J, Yurchenko SN, Furtenbacher T, Császár AG. MARVEL analysis of high-resolution rovibrational spectra of  $^{16}\text{O}^{13}\text{C}^{18}\text{O}$ . *J Comput Chem* 2025;46:e27541. <http://dx.doi.org/10.1002/jcc.27541>.
- [41] Azzam AAA, Azzam SAA, Aburumman KAA, Tennyson J, Yurchenko SN, Császár AG, Furtenbacher T. MARVEL analysis of high-resolution rovibrational spectra of the  $^{18}\text{O}^{12}\text{C}^{18}\text{O}$ ,  $^{17}\text{O}^{12}\text{C}^{18}\text{O}$ , and  $^{18}\text{O}^{13}\text{C}^{18}\text{O}$  isotopologues of carbon dioxide. *J Mol Spectrosc* 2024;405:111947. <http://dx.doi.org/10.1016/j.jms.2024.111947>.
- [42] Mansour MHI, Al-Iter ABI, Azzam AAA, Tennyson J, Furtenbacher T, Császár AG. MARVEL analysis of high-resolution rovibrational spectra of  $^{16}\text{O}^{13}\text{C}^{17}\text{O}$  and  $^{17}\text{O}^{12}\text{C}^{17}\text{O}$ . *J Mol Spectrosc* 2025. submitted for publication.
- [43] Tashkun SA, Perevalov VI, Gamache RR, Lamouroux J. CDS-296, high-resolution carbon dioxide spectroscopic databank: An update. *J Quant Spectrosc Radiat Transfer* 2019;228:124–31. <http://dx.doi.org/10.1016/j.jqsrt.2019.03.001>.
- [44] Tennyson J, Furtenbacher T, Yurchenko SN, Császár AG. Empirical rovibrational energy levels for nitrous oxide. *J Quant Spectrosc Radiat Transfer* 2024;316:108902. <http://dx.doi.org/10.1016/j.jqsrt.2024.108902>.
- [45] Newman MEJ. *Networks*. Oxford: Oxford University Press; 2010.
- [46] Furtenbacher T, Tóbiás R, Tennyson J, Polyansky OL, Császár AG. W2020: A database of validated rovibrational experimental transitions and empirical energy levels of  $\text{H}_2^{16}\text{O}$ . *J Phys Chem Ref Data* 2020;49:033101. <http://dx.doi.org/10.1063/5.0008253>.
- [47] Pavanello M, Adamowicz L, Alijah A, Zobov NF, Mizus II, Polyansky OL, Tennyson J, Szidarovszky T, Császár AG, Berg M, Pettrigiani A, Wolf A. Precision measurements and computations of transition energies in rotationally cold triatomic hydrogen ions up to the mid-visible spectral range. *Phys Rev Lett* 2012;108:023002. <http://dx.doi.org/10.1103/PhysRevLett.108.023002>.
- [48] Furtenbacher T, Szidarovszky T, Fábri C, Császár AG. MARVEL analysis of the rotational–vibrational states of the molecular ions  $\text{H}_2\text{D}^+$  and  $\text{D}_2\text{H}^+$ . *Phys Chem Chem Phys* 2013;15:10181–93. <http://dx.doi.org/10.1039/c3cp44610g>.
- [49] Ritz W. On a new law of series spectra. *Astrophys J* 1908;28:237–43. <http://dx.doi.org/10.1086/141591>.
- [50] Amat G, Pimbert M. On Fermi resonance in carbon dioxide. *J Mol Spectrosc* 1965;16:278–90. [http://dx.doi.org/10.1016/0022-2852\(65\)90123-2](http://dx.doi.org/10.1016/0022-2852(65)90123-2).
- [51] Rothman LS, Young LDG. Infrared energy levels and intensities of carbon dioxide—II. *J Quant Spectrosc Radiat Transfer* 1981;25:505–24. [http://dx.doi.org/10.1016/0022-4073\(81\)90026-1](http://dx.doi.org/10.1016/0022-4073(81)90026-1).
- [52] Toth RA, Brown LR, Miller CE, Malathy Devi V, Benner DC. Spectroscopic database of  $\text{CO}_2$  line parameters: 4300–7000  $\text{cm}^{-1}$ . *J Quant Spectrosc Radiat Transfer* 2008;109:906–21. <http://dx.doi.org/10.1016/j.jqsrt.2007.12.004>.
- [53] McClatchey RA, Benedict WS, Clough SA, Burch DE, Calfee RF, Fox K, Rothman LS, Garing JS. AFCRL atmospheric absorption line parameters compilation. In: Air force cambridge research laboratories. Tech. Rep. AFCRL-TR-73-0096, 1983, URL [https://modis-images.gsfc.nasa.gov/JavaHAWKS/AFCRL\\_AALPC.pdf](https://modis-images.gsfc.nasa.gov/JavaHAWKS/AFCRL_AALPC.pdf).
- [54] Baldacci A, Rinsland CP, Smith MAH, Rao KN. Spectrum of  $^{13}\text{C}^{16}\text{O}_2$  at 2.8  $\mu\text{m}$ . *J Mol Spectrosc* 1982;94:351–62. [http://dx.doi.org/10.1016/0022-2852\(82\)90011-X](http://dx.doi.org/10.1016/0022-2852(82)90011-X).
- [55] McCoy AB, Sibert EL. Perturbative calculations of vibrational ( $J = 0$ ) energy levels of linear molecules in normal coordinate representations. *J Chem Phys* 1991;95:3476–87. <http://dx.doi.org/10.1063/1.460850>.
- [56] Cerezo J, Bastida A, Requena A, Zúñiga J. Rovibrational energies, partition functions and equilibrium fractionation of the  $\text{CO}_2$  isotopologues. *J Quant Spectrosc Radiat Transfer* 2014;147:233–51. <http://dx.doi.org/10.1016/j.jqsrt.2014.06.003>.
- [57] Lemus R, Sánchez-Castellanos M, Pérez-Bernal F, Fernández JM, Carvajal M. Simulation of the raman spectra of  $\text{CO}_2$ : Bridging the gap between algebraic models and experimental spectra. *J Chem Phys* 2014;141:054306. <http://dx.doi.org/10.1063/1.4889995>.
- [58] Bermudez-Montaña M, Lemus R, Pérez-Bernal F, Carvajal M. Comprehensive vibrational analysis of  $\text{CO}_2$  based on a polyad-preserving model. *Eur Phys J D* 2017;71:147. <http://dx.doi.org/10.1140/epjd/e2017-80178-6>.
- [59] Furtenbacher T, Árendás P, Mellau G, Császár AG. Simple molecules as complex systems. *Sci Rep* 2014;4:4654. <http://dx.doi.org/10.1038/srep04654>.